Journal of the Physical Society of Japan
Vol. 78, No. 8, August, 2009, 084724

Electronic Structure of $RNiC_2$ (R = La, Y, and Th)

Izumi HASE[1,2] and Takashi YANAGISAWA[1,2]

[1]*Condensed-Matter Physics Group, Nanoelectronics Research Institute, National Institute of Advanced Industrial Science and Technology, Tsukuba Central 2, 1-1-1 Umezono, Tsukuba, Ibaraki 305-8568*
[2]*CREST, Japan Science and Technology Agency (JST)*

(Received February 13, 2009; accepted June 4, 2009; published August 10, 2009)

The electronic structures of the non-centrosymmetric Ni-based superconductor $LaNiC_2$, and related compounds $YNiC_2$ and $ThNiC_2$ are calculated by the full-potential augmented plane-wave method. In contrast to that in the case of other Ni-based superconductors, there is only one pair of Fermi surfaces taking the spin degree of freedom into account, when holes are slightly doped. The density of states at the Fermi level mainly consists of Ni 3d, but La 5d/Y 4d components are not negligible. Since their crystal structures lack the inversion symmetry, a spin–orbit interaction splits the bands. The splitting values are 3.1 and 2.0 mRy for $LaNiC_2$ and $YNiC_2$, respectively. Using the similarity of the band structures of $LaNiC_2$ and $ThNiC_2$, the Th^{4+} doping dependence of T_c for these compounds can be partly explained by an extended rigid band model.

KEYWORDS: electronic structure, band calculation, FLAPW method, $LaNiC_2$, $YNiC_2$, $ThNiC_2$, superconductivity, non-centrosymmetry, spin–orbit interaction
DOI: 10.1143/JPSJ.78.084724

1. Introduction

Superconductors including magnetic elements are quite interesting for us, because magnetic moments are usually destructive in the normal BCS superconducting state. Nickel-based superconductors have provided us with such interesting examples as $MgCNi_3$,[1] $CdCNi_3$,[2] YNi_2B_2C,[3] and the recently found nickel-pnictide LaNiPO.[4] Among them, $LaNiC_2$ ($T_c = 2.7$ K)[5,6] is interesting because it lacks space inversion symmetry. Since the discovery of $CePtSi_3$,[7] intensive studies have been made for this type of superconductor without inversion symmetry. It is expected that a non-BCS type order will be realized in both magnetic and non-centrosymmetric superconductors. In fact, it is suggested that the superconducting gap of $LaNiC_2$ is nodal.[5] Very recently, it has also been suggested that the time-reversal symmetry of $LaNiC_2$ is broken.[8] On the other hand, there are other experimental data suggesting that the superconductivity in $LaNiC_2$ is "normally BCS-like".[6,9,10] The symmetry of the superconducting order parameter of $LaNiC_2$ is still controversial. The isostructural compound $YNiC_2$ shows superconductivity when the 5f element Th is doped into it. The maximum T_c is $\sim$8.3 K in $(Y_{0.5}Th_{0.5})NiC_2$.[11] However, $YNiC_2$ itself shows no superconductivity down to 0.5 K.[11]

In order to understand the nature of superconductivity in these compounds, it is very important to determine the band structure. However, there have been no reports on the band structure calculation of $LaNiC_2$ and $YNiC_2$, to the best of our knowledge. In this paper, we present results of a first-principles band calculation for $LaNiC_2$ and its isovalent non superconducting compound $YNiC_2$. For help in understanding the Th doping effect, we also calculated the band structure of the hypothetical compound $ThNiC_2$. This paper is organized as follows: In §2, we describe the crystal structure of $RNiC_2$ (R = La, Y, and Th) and details of the calculation. In §3, we present the band properties and provide some discussions.

2. Details of Calculation

To the best of our knowledge, there are no experimental data for the atomic coordinates of $LaNiC_2$ and $YNiC_2$. Therefore, we used the internal atomic parameters of $CeNiC_2$ for $LaNiC_2$, and $DyNiC_2$ for $YNiC_2$.[12] Since the lattice constants of these pairs are quite similar and their maximum difference is below 0.1%, we consider that the results do not depend much on the minor changes of the atomic coordinates. In order to understand the Th doping effect, we also performed calculation for the hypothetical compound $ThNiC_2$. Experimentally, it is known that $(La_{1-x}Th_x)NiC_2$ can be synthesized within $0 \leq x \leq 0.8$.[13] The lattice parameters of $(La_{1-x}Th_x)NiC_2$ ($0 \leq x \leq 0.8$) are measured, and a, b, and the volume $V = abc$ are found to obey Vegard's law. We extrapolated these data to $x = 1$ and found $a = 3.8828$ Å, $b = 4.4691$ Å, and $V = 107.23$ Å^3, and thus $c = 6.1795$ Å. For internal atomic parameters, we used those of $CeNiC_2$ because the ionic radii of Ce^{3+} and Th^{4+} are similar.

The scheme used in our calculations is the standard full-potential augmented plane wave (FLAPW) method. We used the program codes TSPACE[14] and KANSAI-94. For the exchange–correlation potential, we adopted local-density approximation (LDA), according to Gunnarson and Lundqvist.[15] Since there is no magnetic order in $YNiC_2$ and $LaNiC_2$,[16,17] we only performed the calculations in the paramagnetic (not spin-polarized) states.

According to the convention used in TSPACE,[14] we rewrite the original space group Amm2 as $Cm2m$ by replacing the crystal axis from (a, b, c) to (c, a, b). This replacement can clarify the layer structure of the compounds. The La plane is at $z = 0$, and the NiC_2 plane is at $z = 0.5$. They are alternatively stacked. The structural parameters we used are described in Table I. The muffin-tin (MT) radii are set to $0.27a$ for La/Y/Th, $0.23a$ for Ni, $0.14a$ for C, where a is the (new) lattice constant 4.564 Å. For plane basis functions, we used about 450 LAPWs.

Table I. Structural parameters of $LaNiC_2$ and $YNiC_2$ used in this calculation. We assumed that $LaNiC_2$ and $YNiC_2$ have atomic coordinates of $CeNiC_2$[21] and $DyNiC_2$,[21] respectively. For the lattice parameters, we used the experimental values.[12]

	a (Å)	b (Å)	c (Å)				
$LaNiC_2$	4.564	6.204	3.959	La/Th(2a)	$(0, y, 0)$	$y = 0.9936$	
$ThNiC_2$	4.4691	6.1795	3.8828	Ni(2b)	$(0, y, 1/2)$	$y = 0.608$	
				C(4e)	$(x, y, 1/2)$	$x = 0.155$	$y = 0.285$
$YNiC_2$	4.509	6.239	3.562	Y(2a)	$(0, y, 0)$	$y = 0.0$	
				Ni(2b)	$(0, y, 1/2)$	$y = 0.6116$	
				C(4e)	$(x, y, 1/2)$	$x = 0.1523$	$y = 0.3016$

Since this space group lacks inversion symmetry, the inclusion of the spin–orbit interaction (SOI) may be important for understanding the band structure. SOI is included within the second-variational procedure.[18] Self-consistent potentials are calculated at 60 uniformly distributed k-points in the irreducible Brillouin zone (IBZ, 1/8th of the BZ). The density of states (DOS) and the number of carriers are deduced from the eigenstates at 369 uniformly distributed points in the same IBZ by the ordinary tetrahedron method.

3. Results and Discussion

3.1 $LaNiC_2$

The energy band dispersion without SOI is shown in Fig. 1 along the principal symmetry axes in the Brillouin zone. All the bands are doubly degenerate because of the spin degrees of freedom. The states in the energy ranges of -0.3 to -0.2 Ry and 0.2 to 0.3 Ry mainly consist of La 5p and C 2s orbitals, respectively. The states in the energy range of 0.3–0.7 Ry mainly consist of C 2p and Ni 3d orbitals. Above ~0.7 Ry, strongly mixed Ni 3d and La 5d states are found. The condensed bands along 0.8–0.9 Ry are mainly La 4f states.

To determine the effect of SOI in this compound, we plot the bands that are very near the Fermi level in Fig. 2. At the points Γ, Y, Z, T, R, S and at the points along the axes B and Δ, these bands degenerate because of the high symmetry of the k-point, but at the other k-points the degeneracy is lifted because of the lack of space inversion symmetry. Nevertheless, $E(-k) = E(k)$ is guaranteed by the time reversal symmetry of the Hamiltonian. As we can see, the magnitude of SOI is not so large. The maximum value of the splitting of the 14th band is 13.5 mRy at approximately $A(5/8, 0, 1/2)$, and the average value in the IBZ is $E_{so}^{av} = 3.1$ mRy. This is about half of the value of the splitting in $CePtSi_3$,[19] and is comparable to the Debye temperature $\theta_D = 496$[5] or 388 K.[6] This is because the main component of this band is the Ni 3d state, instead of the Ce 4f state in $CePtSi_3$. Nevertheless, the ratio of E_{so}^{av} to the superconducting gap Δ_{SC} is $E_{so}^{av}/\Delta_{SC} = 72$, if we assume a moderate ratio $2\Delta_{SC}/k_B T_c = 5$. Thus we can conclude that the "strong-SOI limit" treatment by Samokhin *et al.*[19] is essentially correct, at least, as a first approximation.

The Fermi surfaces (FSs) of $LaNiC_2$ are shown in Fig. 3. There are only two FSs when we neglect SOI. The 14th band is nearly half-filled, and the 15th band gives a small electron pocket around the Z point. This small electron pocket may easily be eliminated by hole doping (namely, 0.28% doping, see below), for example, Sr doping for a La site. In the recently found superconductor LaFe(O,F)As, a small hole pocket at Z point is eliminated when the electrons are doped. The numbers of electrons in the 14th and 15th bands are 0.9972 and 0.0028, respectively. After the inclusion of SOI, the 14th band splits and contains 0.5314 and 0.4659 electrons, and the 15th band splits and contains 0.0016 and 0.0011 electrons. All these bands show a large dispersion along the c-axis, suggesting a large transfer integral between the NiC_2 layers via a La layer.

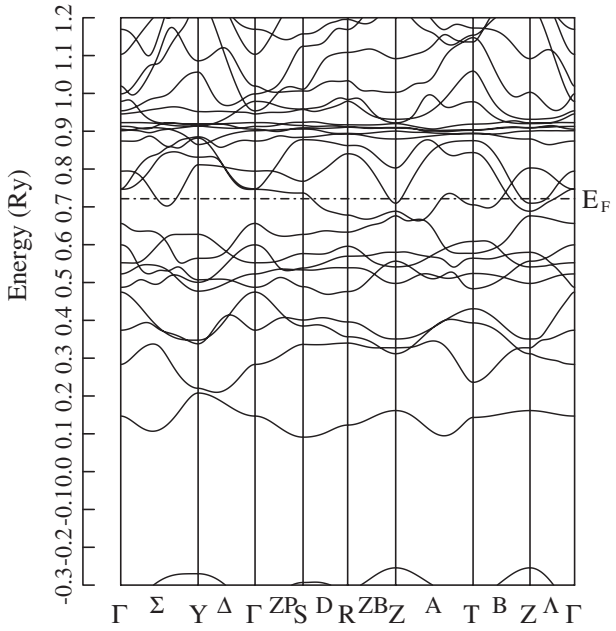

Fig. 1. Energy bands of $LaNiC_2$ without SOI. The symbols ZP and ZB denotes the axes $(k, k, 0)$ and $(k, k, 1/2)$, respectively. Other symbols are the same as the standard notations, see refs. 14 and 22.

The DOS's of $LaNiC_2$ are shown in Fig. 4. In this wide energy range, the effect of SOI is very small except for the splitting of La 4f bands to the $4f_{7/2}$ and $4f_{5/2}$ complexes. The DOS at the Fermi level $D(E_F)$ is 33.1 states/Ry, which gives a calculated specific heat coefficient $\gamma_{cal} = 5.73$ mJ/(mol·K^2). The experimental observed value is $\gamma_{exp} = 7.83$[5] or 6.5 mJ/(mol·K^2),[6] then the enhancement factor $\lambda = 1.36$ or 1.13 is not so large. It is known that the T_c of $LaNiC_2$ increases when the 5f element Th is used as dopant. The maximum T_c is ~7.9 K in $(La_{0.5}Th_{0.5})NiC_2$.[11] If we adopt a rigid band model, and assume that the number of electrons donated by the Th atom is larger than that donated by the La atom by 1, then the E_F of $(La_{0.5}Th_{0.5})NiC_2$ is shifted to form the right vertical dotted line in Fig. 4. In $LaNiC_2$, E_F is already at the peak of DOS, and further electron doping (and also hole doping) may decrease $D(E_F)$, and thus decrease T_c. We discuss this point in §3.3.

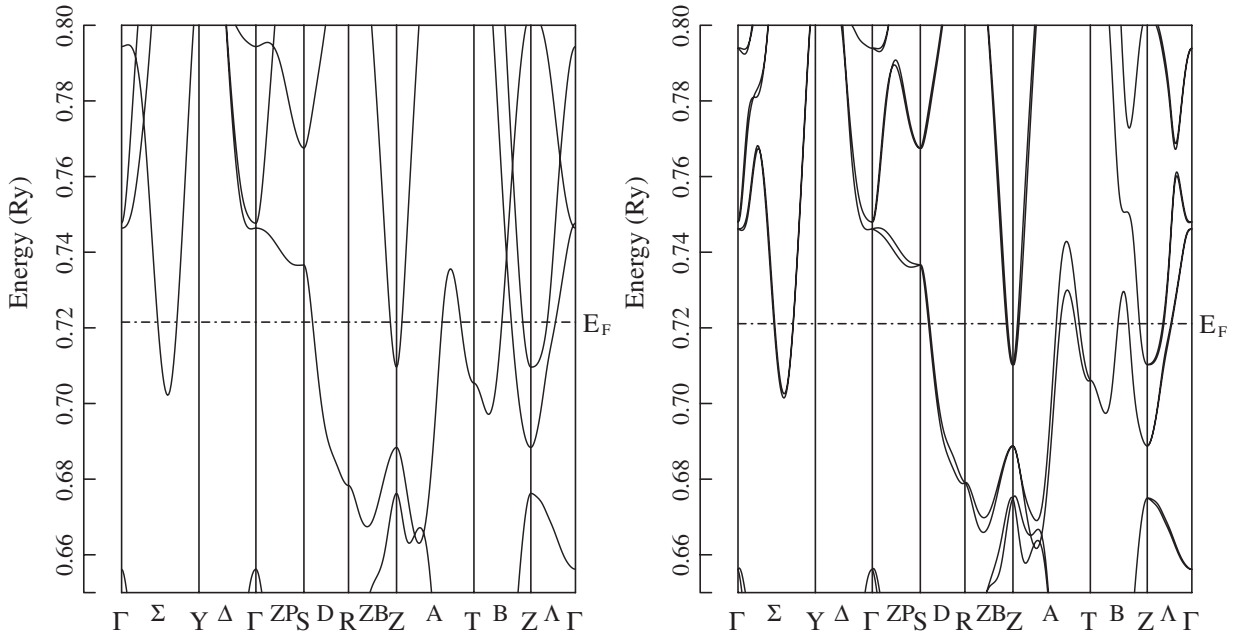

Fig. 2. Energy bands of $LaNiC_2$ (a) without and (b) with SOI near E_F.

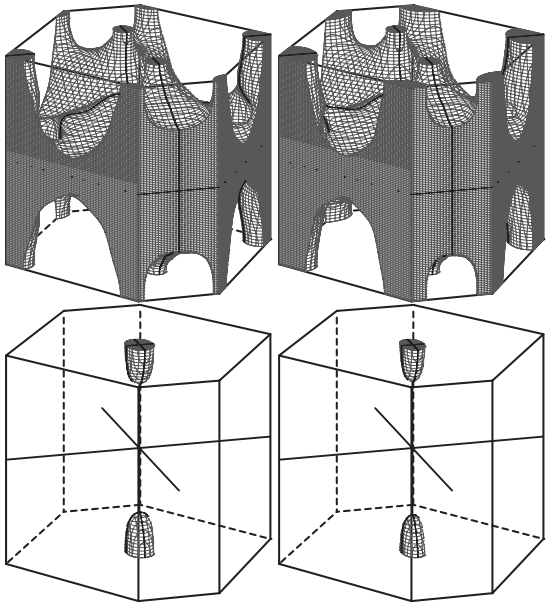

Fig. 3. FSs of $LaNiC_2$ after inclusion of SOI. Large FSs are the 27th and 28th electron surfaces, which come from the 14th electron surface without SOI. Small pockets are the 29th and 30th hole surfaces, which come from the 15th hole surface without SOI.

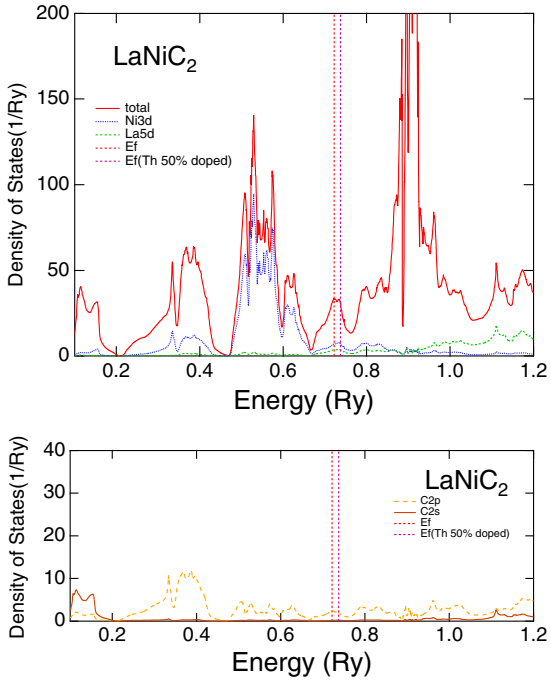

Fig. 4. (Color online) DOS's of $LaNiC_2$ after inclusion of SOI. The left and right vertical lines show the E_F values in nondoped and 50%-Th-doped cases.

3.2 *YNiC$_2$*

The energy band dispersions of $YNiC_2$ with and without SOI near E_F are shown in Fig. 5. The overall feature in the wide energy range is similar to that of $LaNiC_2$ (not shown). The bands near E_F are also similar between $LaNiC_2$ and $YNiC_2$, but in $YNiC_2$ the conduction band does not dip in E_F along the Γ–Σ–Y direction. The maximum value of the splitting of the 14th band is 6.2 mRy at approximately YP$(3/8, 0, 1/16)$, and the average value in the IBZ is $E_{so}^{av} = 2.0$ mRy. The decrease in the value from $LaNiC_2$ is partly due to the strong hybridization between the Ni 3d and La 5d/Y 4d states near E_F, and partly due to the absence of 4f electrons.

The Fermi surfaces of $YNiC_2$ without SOI are shown in Fig. 6. The value of the splitting of the FSs by SOI is too small to change the shape of FSs, which is almost similar to that of $LaNiC_2$. Again there are two FSs without SOI: one is almost half-filled and the other is a small electron pocket around the Z point. The numbers of electrons in each band are 0.9903 and 0.0097, respectively. After the inclusion of SOI, the 14th band splits and contains 0.5052 and 0.4849 electrons, and the 15th band splits and contains 0.0057 and 0.0041 electrons. The differences in the number of electrons between the split bands are also smaller than that in $LaNiC_2$, again due to the smaller splitting value of the bands by SOI.

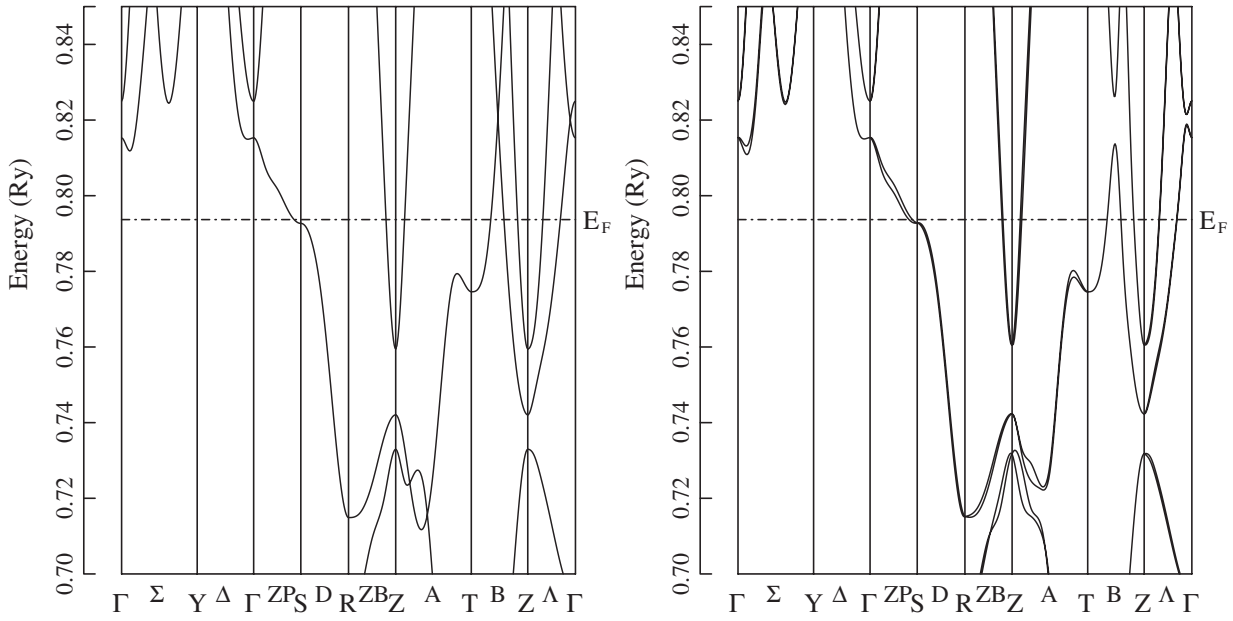

Fig. 5. Energy bands of $YNiC_2$ (a) without and (b) with SOI near E_F.

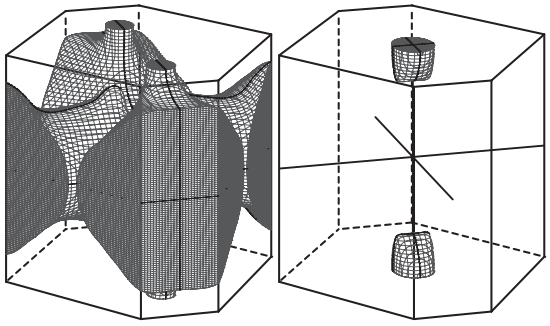

Fig. 6. 13th and 14th FSs of $YNiC_2$ before inclusion of SOI. The 14th band is written in a hole picture.

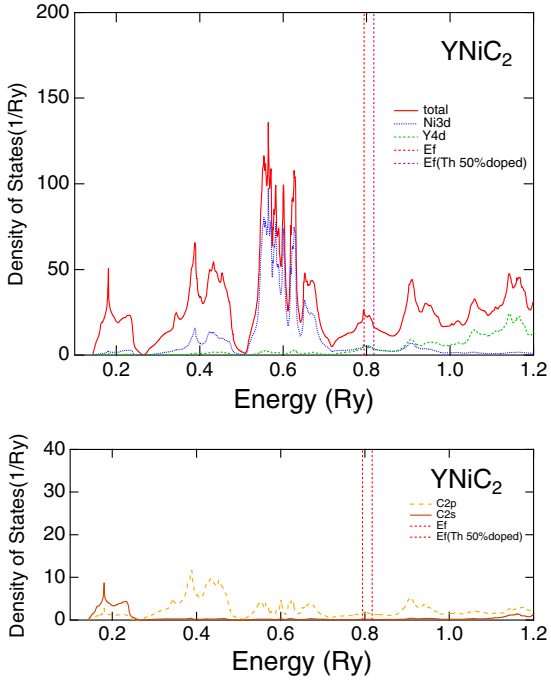

Fig. 7. (Color online) DOS's of $YNiC_2$ after inclusion of SOI. The left and right vertical lines show the E_F values of nondoped and 50%-Th-doped case.

The DOS's of $YNiC_2$ are shown in Fig. 7. The overall feature is almost the same except for the absence of the La 4f peak. The DOS's of $LaNiC_2$ are shown in Fig. 4. The DOS at the Fermi level $D(E_F)$ is 25.2 Ry^{-1}, which gives a calculated specific heat coefficient $\gamma_{cal} = 4.36\,mJ/(mol{\cdot}K^2)$. Experimental data of the specific heat is available for $(Y_{0.5}Th_{0.5})NiC_2$, that is, $\gamma_{exp} = 11.04\,mJ/(mol{\cdot}K^2)$.[11] If we adopt a rigid band model again, and assume that the Th atom donates one more electron than Y, then E_F is shifted in the right vertical dotted line in Fig. 7. Here, $D(E_F^{cal,doped})$ is 16.7 Ry^{-1}, which gives $\gamma_{cal,doped} = 2.89\,mJ/(mol{\cdot}K^2)$. The enhancement factor $\lambda = \gamma_{exp}/\gamma_{cal,doped} = 3.82$ is very large. Moreover, DOS monotonically decreases in this energy region, which is in contrast to the increase in T_c with increasing Th content. These findings suggest that the assumed rigid band model may not be appropriate. We discuss this point in the next subsection.

3.3 *ThNiC$_2$*

We show the results for $ThNiC_2$. The DOS and $E(k)$ curves are shown in Figs. 8 and 9. One can see that the shapes of the DOS and $E(k)$ curves are similar to those of $LaNiC_2$ and $YNiC_2$. This result supports our treatment of the rigid band model for the Th doping effect on $LaNiC_2$ and $YNiC_2$, at least qualitatively. Since the number of valence electrons of $ThNiC_2$ is one more than those of $LaNiC_2$ and $YNiC_2$, E_F is shifted to a higher energy. $D(E_F)$ becomes 19.8 Ry^{-1}, and this is larger than the rigid band model for $LaNiC_2$ (add one electron to $LaNiC_2$), 13.8 Ry^{-1}. As for $(Y_{0.5}Th_{0.5})NiC_2$, we can also assume that 50% of holes are doped into $ThNiC_2$. In this case, $D(E_F)$ becomes 31.0 Ry^{-1}, almost twice as large as the above value of 16.7 Ry^{-1}, assuming that 50% of electrons are doped into $YNiC_2$. The maximum value of the splitting of the 14th band is 42 mRy at approximately A(5/8, 0, 1/2), and the average value in the IBZ is $E_{so}^{av} = 8.8$ mRy. These very large SOI splitting values

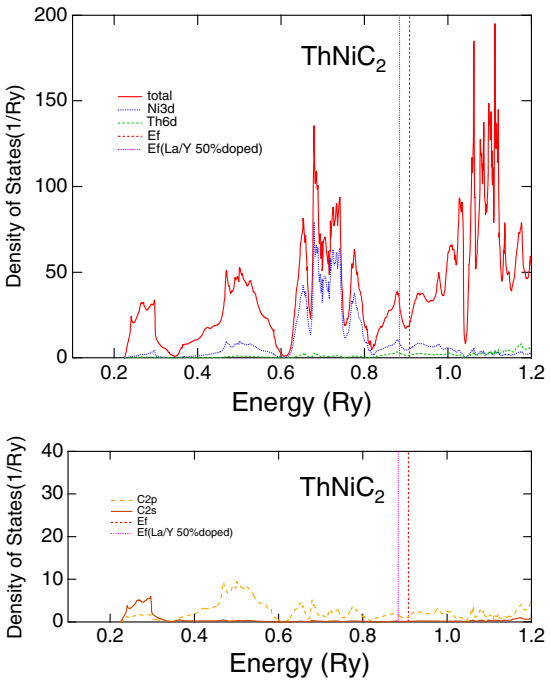

Fig. 8. (Color online) DOS's of $ThNiC_2$ after inclusion of SOI. The left and right vertical lines show E_F of nondoped and 50% La(Y) doped case.

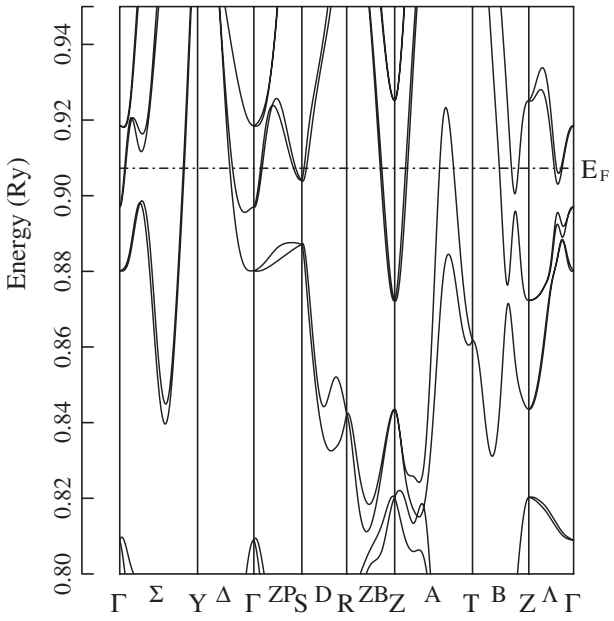

Fig. 9. Energy bands of $ThNiC_2$ with SOI near E_F.

come from the Th 5f component. Since the Th 5f orbitals are more expanded than the La 4f orbitals, they can easily hybridize with the Ni 3d bands. The Th 5f partial DOS at E_F in $ThNiC_2$ is $2.2\,Ry^{-1}$ (11% of the total DOS), whereas the La 4f partial DOS at E_F is $1.1\,Ry^{-1}$ (3.3% of the total DOS). The FSs of $ThNiC_2$ are shown in Fig. 10. Since the number of valence electrons of $ThNiC_2$ is one more than that of $LaNiC_2$, hole FSs shrink and electron FSs expand. Moreover, two small electron FSs appear. Reflecting the large SOI splitting value at $A(5/8, 0, 1/2)$, the shapes of the 27th and 28th FSs are significantly different.

Finally, we consider the Th-doping effects on $LaNiC_2$ and $YNiC_2$. In the above subsections, we have already seen that the simplest rigid-band model starting from $LaNiC_2$ and $YNiC_2$ fails to describe the doping dependence of T_c. Evidently, the opposite picture, i.e., the rigid-band model starting from $ThNiC_2$, also does not work, because it gives the same curve $T_c(x)$ for La- and Y-doped compounds, in contrast to the experimental findings.[11,13] Since the DOS curves of these compounds are not very different, we assume the following "extended" rigid-band model for $(La_{1-x}Th_x)NiC_2$ as

$$D(x, E_F(x)) = (1-x)D(La, E_F(x)) + xD(Th, E_F(x)), \quad (1)$$

where $D(La, E_F(x))$ and $D(Th, E_F(x))$ denote the DOS curves of $LaNiC_2$ and $ThNiC_2$, respectively. $E_F(x)$ is determined so

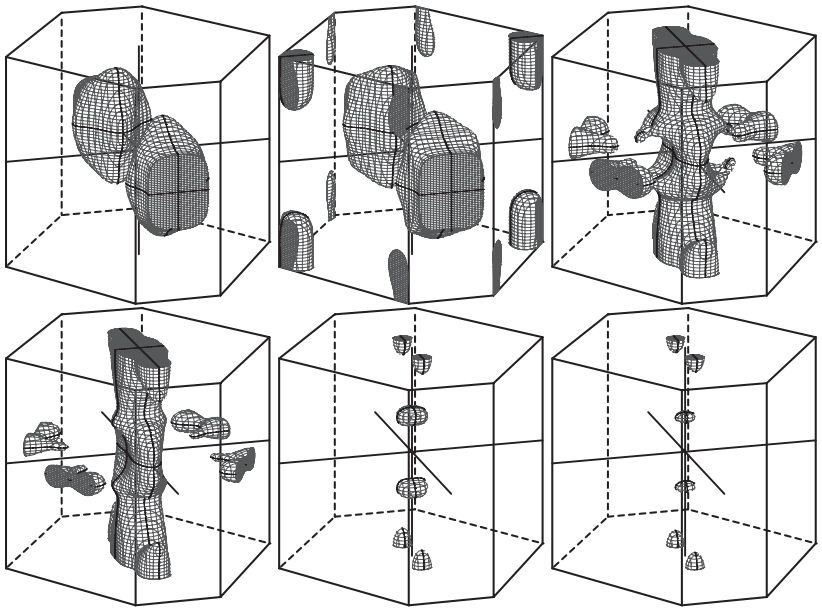

Fig. 10. FSs of $ThNiC_2$ after inclusion of SOI. The two upper left panels are the 27th and 28th hole FSs. The other panels are the 29th, 30th, 31st, and 32nd electron FSs.

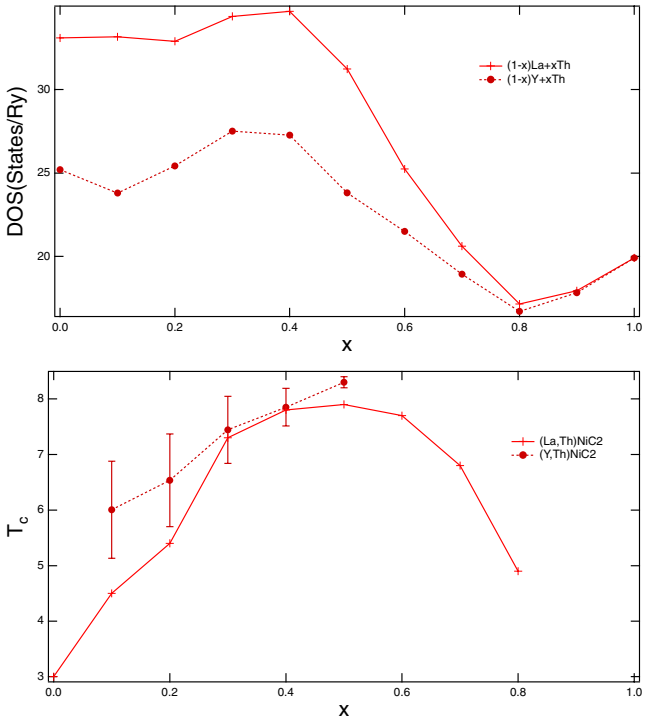

Fig. 11. (Color online) (a) DOS's at E_F values of $(La_{1-x}Th_x)NiC_2$ and $(Y_{1-x}Th_x)NiC_2$ estimated using the extended rigid-band model. (b) Experimental T_c values of $(La_{1-x}Th_x)NiC_2$[13] and $(Y_{1-x}Th_x)NiC_2$.[11] In both panels, the solid lines are for the La system and the dashed lines are for the Y system. For the La system, we used $T_{c,\rho=0}$, and for the Y system we used T_c^{mid}. Error bars denote the 10 and 90% values.

that the number of valence electrons becomes correct, as in the ordinary rigid-band model. If we set the first (second) term on the right-hand side as zero, we obtain the ordinary rigid-band model starting from $ThNiC_2$ ($LaNiC_2$). Note that at $x = 0$ or $x = 1$, i.e., at both end members, we obtain the correct DOS using the above equation. Similarly, we can obtain the DOS at the E_F of $(Y_{1-x}Th_x)NiC_2$ with replacing La by Y in the above equation. We plot DOS versus x in Fig. 11, and compare T_c between Th-doped $LaNiC_2$ and $YNiC_2$.[11,13] We can see that the peak position of T_c and the decrease in T_c in the doping range $0.5 < x < 0.8$ are well reproduced by this model. However, the increase in T_c in the doping range $0 < x < 0.5$ is not well reproduced.[20] We also cannot explain this behavior of T_c by the "isotope effect" due to the difference in mass between the La and Th atoms, because Th is heavier than La, and this substitution may decrease T_c. The disagreement between the theory and the experiment is worse in $(Y_{1-x}Th_x)NiC_2$ than in $(La_{1-x}Th_x)NiC_2$, maybe because the change in the lattice parameter is larger in $(Y_{1-x}Th_x)NiC_2$, which brings about some modifications to the band structure. One scenario for elucidating this behavior is as follows: In $LaNiC_2$, an exotic superconducting order parameter exists, as suggested by some experiments.[5,8] In the Th-rich region, the normal BCS mechanism may work because the exotic superconductivity is weak for disorder in most cases. In the La-rich region, these two (exotic and normal) order parameters compete, thus, T_c deviates from the (extended) rigid-band model.

In summary, we have calculated the electronic structures of $LaNiC_2$ and $YNiC_2$ by the FLAPW method. The lack of an inversion center in these crystals leads to the splitting of the bands due to a spin–orbit interaction, and the value of this splitting is 3.1 mRy in $LaNiC_2$. This is about half of that in $CePtSi_3$, and is comparable to the Debye temperature. For $YNiC_2$ the value of this splitting is 2.0 mRy. These small splitting values compared with those in $CePtSi_3$ are due to the small SOI of Ni 3d orbitals, which is the main component near the Fermi level. Both compounds have one half-filled band and one small electron pocket. The doping dependence of $(La_{1-x}Th_x)NiC_2$ is partly explained by the extended rigid-band model.

Acknowledgment

We thank T. Shimomura for valuable discussions and encouragement.

1) T. He, Q. Huang, A. P. Ramire, Y. Wang, K. A. Rega, N. Rogado, M. A. Hayward, M. K. Haas, J. S. Shusky, K. Inumara, H. W. Zandbergen, N. P. Ong, and R. J. Cava: Nature (London) **411** (2001) 54.
2) M. Uehara, T. Yamazaki, T. Kôri, T. Kashida, Y. Kimishima, and I. Hase: J. Phys. Soc. Jpn. **76** (2007) 034714.
3) R. J. Cava, H. Takagi, H. W. Zandbergen, J. J. Krajewski, W. F. Peck, Jr., T. Siegrist, B. Batlogg, R. B. Van Dover, R. J. Felder, K. Mizuhashi, J. O. Lee, H. Eisaki, and S. Uchida: Nature (London) **367** (1994) 252.
4) T. Watanabe, H. Yanagi, T. Kamiya, Y. Kamihara, H. Hiramatsu, M. Hirano, and H. Hosono: Inorg. Chem. **46** (2007) 7719.
5) W. H. Lee, H. K. Zeng, Y. D. Yao, and Y. Y. Chen: Physica C **266** (1996) 138.
6) V. K. Pecharsky, L. L. Miller, and K. A. Gschneider: Phys. Rev. B **58** (1998) 497.
7) E. Bauer, G. Hilscher, H. Michor, Ch. Paul, E. W. Scheidt, A. Gribanov, Yu. Seropegin, H. Noël, M. Sigrist, and P. Rogl: Phys. Rev. Lett. **92** (2004) 027003.
8) A. D. Hillier, J. Quintanilla, and R. Cywinskii: Phys. Rev. Lett. **102** (2009) 117007.
9) Y. Iwamoto, Y. Iwasaki, K. Ueda, and T. Kohara: Phys. Lett. A **250** (1998) 439.
10) H. H. Sung, S. Y. Chou, K. J. Syu, and W. H. Lee: J. Phys.: Condens. Matter **20** (2008) 165207.
11) K. J. Syu, H. H. Sung, and W. H. Lee: Solid State Commun. **141** (2007) 519.
12) W. Jeitschko and M. H. Gerss: J. Less-Common Met. **116** (1986) 147.
13) W. H. Lee and H. K. Zeng: Solid State Commun. **101** (1997) 323.
14) A. Yanase: *Fortran Program for Space Group (TSPACE)* (Shokabo, Tokyo, 1995) [in Japanese].
15) O. Gunnarson and B. I. Lundqvist: Phys. Rev. B **13** (1976) 4274.
16) P. Kotsanidis, J. K. Yakinthos, and E. Gamari-Seale: J. Less-Common Met. **152** (1989) 287.
17) Y. Koshikawa, H. Onodera, M. Kosaka, H. Yamauchi, M. Ohashi, and Y. Yamaguchi: J. Magn. Magn. Mater. **173** (1997) 72.
18) D. D. Koelling and B. N. Harmon: J. Phys. C **10** (1977) 3107.
19) K. Samokhin, E. S. Zijlstra, and S. K. Bose: Phys. Rev. B **69** (2004) 094514.
20) In the standard BCS model, $T_c = 1.14\hbar\omega_D \exp(-1/DV)$, where ω_D is the Debye temperature, D is the DOS at E_F, and V is the attractive interaction between the two electrons. This leads to $\log T_c = -1/DV + \text{const.}$, i.e., $\log T_c$ and $-1/D$ show a linear relation. However, we have confirmed that the x dependence of these quantities is essentially the same as that in Fig. 11.
21) O. I. Boduk and E. P. Marusin: J. Dokl. Akad. Nauk Ukr. SSR, Ser. A **41** (1979) 1048.
22) C. J. Bradley and A. P. Cracknell: *The Mathematical Theory of Symmetry in Solids* (Clarendon Press, Oxford, U.K., 1972) p. 98.